Transmission-mode GaN photocathode based on graded $Al_xGa_{1-x}N$ buffer layer

Xiaoqing Du (杜晓晴)[1*], Benkang Chang (常本康)[2], Yunsheng Qian (钱芸生)[2], and Pin Gao (高 频)[2]

[1]*Key Laboratory of Optoelectronic Technology and Systems of Ministry of Education of China, College of Optoelectronic Engineering, Chongqing University, Chongqing 400044, China*

[2]*Institute of Electronic Engineering and Opto-Electric Technology, Nanjing University of Science and Technology, Nanjing 210094, China*

**Corresponding author: duxq@cqu.edu.cn*

Received July 5, 2010; accepted August 3, 2010; posted online January 1, 2011

We create a GaN photocathode based on graded $Al_xGa_{1-x}N$ buffer layers to overcome the influence of buffer-emission layer interface on the photoemission of transmission-mode GaN photocathodes. A gate-shaped spectral response with a 260-nm starting wavelength and a 375-nm cut-off wavelength is obtained. Average quantum efficiency is 15% and short wavelength responses are almost equivalent to long wavelength ones. The fitted interface recombination velocity is 5×10^4 cm/s, with negligible magnitude, proving that the design of the graded buffer layers is efficient in obtaining good interface quality between the buffer and the emission layer.

OCIS codes: 040.7190, 160.1890, 230.0040, 260.7210.

doi: 10.3788/COL201109.010401.

Numerous civilian and military applications have pushed forward the development of ultraviolet (UV) detectors[1,2]. In recent years, the GaN UV photocathode has been widely explored for its high-efficiency detection, low dark current, high UV/visible rejection ratio, good stability, and concentrated energy distribution of photoelectrons[3−7]. Although the top quantum efficiency (QE) of the reflection-mode GaN photocathode of 70% has been obtained[7], we are still a long way from putting the GaN photocathode to practical use, and are yet to develop transmission-mode GaN photocathodes[5−7]. The transmission-mode photocathode is the type commonly used in practical applications. The incident radiation is detected on the back of the photocathode, and the induced photoelectrons are emitted from the front surface of the cathode.

The schematic of the transmission and reflection photocathode operation is shown in Fig. 1. Transmission-mode photocathodes can be combined with electron multiplier devices to form photomultiplier tubes (PMTs), imaging intensifiers, or other vacuum detection devices for low-level UV detection.

Sapphire-AlN buffer layer-GaN emission layer is a commonly used material structure for transmission-mode GaN photocathodes[5−7]. Both sapphire and AlN are transparent for UV radiation and have good mechanical supporting capacity. However, their structures are not ideal. A high degree of lattice mismatch exists between AlN and GaN due to the large difference of their lattice constants. The lattice mismatch causes large lattice defects, such as dislocations, at the interface of AlN and GaN during GaN material growth. These defects form interface recombination centers and capture photoelectrons generated near the interface, resulting in a great decline in photoemission efficiency. The diagram of the interface effect on transmission-mode photocathode photoemission is shown in Fig. 2. The typical QE of transmission-mode GaN photocathodes based on AlN buffers is only 3%–5%[7], which is lower than the QE of 10% of the transmission CsTe photocathode[3]. To obtain high-performance transmission-mode GaN photocathode, a high quality interface between buffer layer and GaN layer is needed.

In this letter, graded $Al_xGa_{1-x}N$ buffer layers are presented to improve the interface quality of transmission-mode GaN photocathodes. The overall structure of the GaN photocathode material is shown in Fig. 3(a), and the specific structure of the buffer layer is shown in Fig. 3(b). The photocathode consists of a sapphire substrate, graded p-type $Al_xGa_{1-x}N$ buffer layers, and p-type GaN emission layers. The sapphire substrate is c-plane, double-polished, with a thickness of 300–500 μm. Graded $Al_xGa_{1-x}N$ buffer layers are epitaxially grown on the sapphire substrate by metal organic chemical vapor deposition (MOCVD). In buffer layers, the Al mole fraction decreases gradually from bottom (substrate) to top, and finally transits into the GaN emission layer naturally.

$Al_xGa_{1-x}N$ materials are ternary compounds of the GaN material and their lattice constant is slightly smaller than that of the GaN material. Using $Al_xGa_{1-x}N$ as buffer material decreases the chances of lattice mismatch at the interface between buffer and emission layer. In addition, the graded design allows the lattice constant of $Al_xGa_{1-x}N$ to decrease gradually with the decline of the

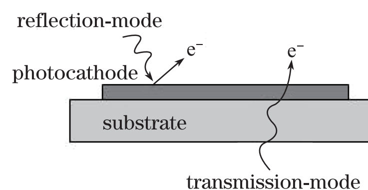

Fig. 1. Schematic of the transmission and reflection photocathode operation.

 © 2011 Chinese Optics Letters

Al composition, ultimately matching the GaN emission material which gradually releases interfacial stress during growth and improves interface quality.

The total number n of $Al_xGa_{1-x}N$ graded layers can be adjusted according to the actual demands and technique levels. In our design, n is four in order to obtain a significant gradient and to facilitate preparation. The thickness of each graded layer is less than 50 nm to ensure the complete release of the lattice stress, and the total thickness is 200 nm to minimize the short wavelength UV absorption by the buffer layers. The minimum Al fraction is designed to be 0.55, making the buffer adsorption wavelength short enough and ensuring that most UV light will be absorbed by the GaN emission layer.

The p-type GaN emission layer is epitaxially grown on the buffer layer by MOCVD. Its doping atom is Mg and the doping concentration is about 3×10^{18} cm^{-3}. The thickness of the GaN emission layer is about 150 nm to match the electron diffusion length and the UV absorption length of p-type GaN materials. This design ensures that long and short wavelength UV can be fully absorbed by the GaN emission layer to generate a significant photoemission effect.

The UV transmission spectra of the photocathode material are shown in Fig. 4. There are five interference peaks in the 380–650 nm range, which correspond to the secondary interferences caused by the GaN epitaxial layer and the four buffer layers. There are two interference peaks in the 650–1000 nm range, caused by the first interferences of the GaN epitaxial layer and the buffer layers.

Preparation of the GaN photocathode consists of surface cleaning and surface activation. The sample was chemically cleaned using pirana acid (H_2SO_4:H_2O_2) bath to remove surface oil and other contaminants. The sample was then loaded into an ultra-high-vacuum (UHV) chamber for heat cleaning and activation. It was heated

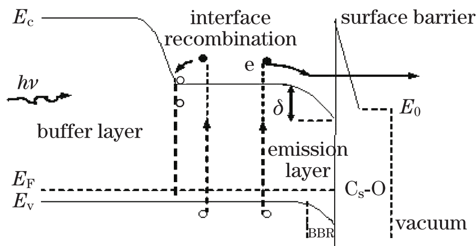

Fig. 2. Diagram of interface effect on transmission-mode photocathode photoemission. E_c: conduction band; E_F: Fermi level; E_v: valence band; E_0: vacuum level; e: electron; δ: amount of band bending; $h\nu$: photon energy; BBR: band bending region.

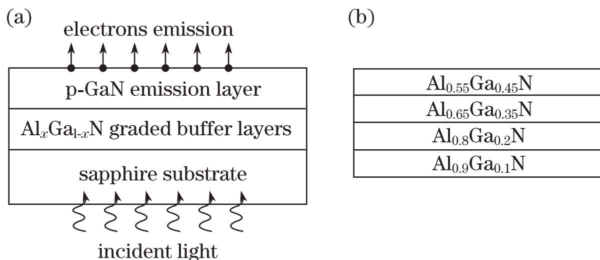

Fig. 3. Structure of transmission-mode GaN photocathode material. (a) Overall structure; (b) specific structure of buffer layer.

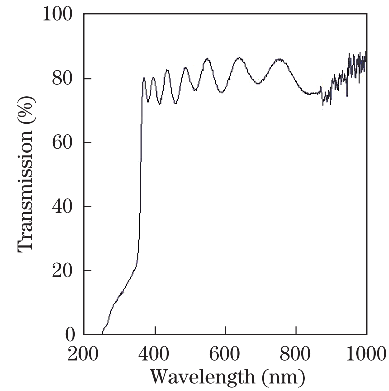

Fig. 4. Transmission spectra of GaN photocathode material.

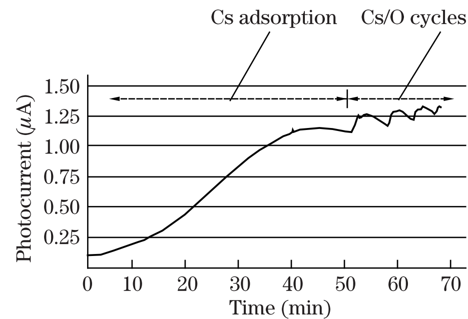

Fig. 5. Activation process of GaN photocathode.

and annealed at 700 °C to remove C, O, and other impurities on the GaN surface, ensuring the atomic-level cleanliness of the surface. Base pressures of the UHV chamber were kept higher than 10^{-6} Pa during the whole cleaning process. The GaN surface was then treated using (Cs,O) activation technique to achieve a negative electron affinity (NEA) state[8,9]. A 10-W/240-V deuterium lamp irradiated the sample surface through the quartz incident window of the UHV chamber to monitor the photocurrent during the (Cs,O) activation process. Photocurrent signal from the photocathode was measured using a current collecting circuit and the photocurrent change during activation was recorded on-line. Activation process of the GaN photocathode is shown in Fig. 5. The photocurrent began to appear at the beginning of Cs adsorption and increased at a steady rate with cessation time. The photocurrent remained unchanged and began to decline slightly, indicating that sufficient amounts of Cs had been adsorbed on the GaN surface and that the cessation was complete. Next, Cs/O cycles were performed to further lower the surface electron affinity and increase the photocurrent. The whole activation process ended after two to three Cs/O cycles.

The QE of the transmission-mode GaN photocathode was measured using UV spectral response on-line test technology. The measured result is shown in Fig. 6. For comparison, Fig. 6 also shows the QE curves of the transmission-mode GaN photocathode based on AlN buffers[7], and the CsTe UV photocathode[3] which was developed earlier and has a positive electron affinity surface.

Results show that the prepared GaN photocathode has obvious gate-shaped and flat spectral responses with a starting wavelength of ~260 nm and a cut-off wavelength

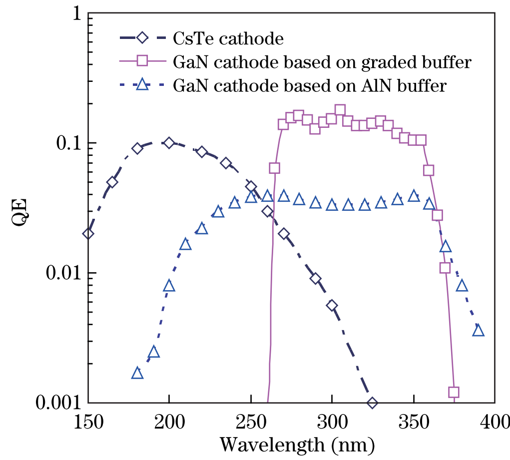

Fig. 6. QE characteristics of different GaN photocathodes.

of 375 nm. The starting wavelength is determined by the interband absorption of the $Al_{0.55}Ga_{0.45}N$ buffer layer, and the cut-off wavelength corresponds to the absorption threshold of the GaN emission layer. Most of the light with a wavelength less than 260 nm is absorbed by the buffer layer because light absorption increases with the Al content of buffer layers and moves toward short wavelengths. Few of the induced photoelectrons in the buffer layer can reach the GaN surface due to the thick buffer layer. Therefore, spectral responses at wavelengths less than 260 nm are very small. When the incident light wavelength is longer than 260 nm, the $Al_xGa_{1-x}N$ buffer layer becomes transparent in the absence of strong interband absorption, and most of the light is absorbed by the GaN emission layer. Most of the induced photoelectrons in the GaN layer can reach the GaN surface because the thickness of the GaN emission layer suits the electron diffusion length. Therefore, spectral responses at wavelengths more than 260 nm become much greater and flat. The average QE within the response waveband is 15%, which is much higher than the 5% top QE of the GaN photocathode based on AlN buffer, and also higher than the 10% QE of the CsTe photocathode. The long wavelength UV response has a steep cut-off, and the short wavelength responses of our prepared GaN photocathode are almost equivalent to the long wavelength ones. UV peak QE at 310 nm is 18%, and dark QE at 370 nm is 0.1%. The UV-visible rejection ratio is higher than 10%.

As shown in Figs. 1 and 2, interface characteristics will directly affect UV response in the transmission operation. The greater the interface recombination velocity, the faster the photoemission efficiencies fall. The relationship between interface recombination velocity and QE for transmission-mode GaN photocathodes can be expressed as[10]

$$Y_{tb}(\lambda) = \frac{P\cdot(1-R)\cdot\alpha L_{\mathrm{D}}}{\alpha^2 L_{\mathrm{D}}^2-1}\times\left\{\frac{\alpha D_n + S_v}{(D_n/L_{\mathrm{D}})\cdot\cosh(T_{\mathrm{e}}/L_{\mathrm{D}}) + S_v\cdot\sinh(T_{\mathrm{e}}/L_{\mathrm{D}})} - \frac{\exp(-\alpha T_{\mathrm{e}})\cdot[S_v\cdot\cosh(T_{\mathrm{e}}/L_{\mathrm{D}}) + (D_n/L_{\mathrm{D}})\cdot\sinh(T_{\mathrm{e}}/L_{\mathrm{D}})]}{(D_n/L_{\mathrm{D}})\cdot\cosh(T_{\mathrm{e}}/L_{\mathrm{D}}) + S_v\cdot\sinh(T_{\mathrm{e}}/L_{\mathrm{D}})} - \alpha L_{\mathrm{D}}\cdot\exp(-\alpha T_{\mathrm{e}})\right\}, \quad (1)$$

where P is the electron surface escape probability, R is the total reflectivity of the substrate and the buffer, α is the adsorption coefficient of the emission material, L_{D} is the electron diffusion length of the emission material, D_n is the electron diffusion coefficient, T_{e} is the thickness of the emission layer, and S_v is the interface recombination velocity between the buffer and the emission layers. The diagram of the influence is shown in Fig. 7.

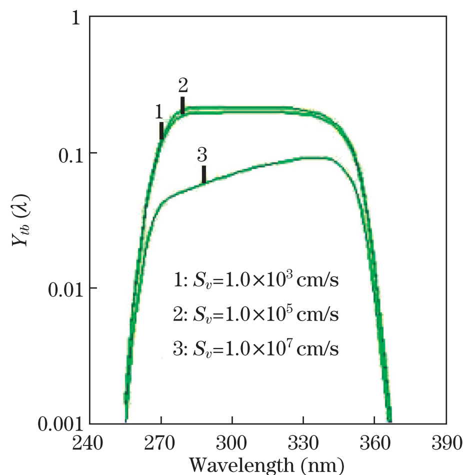

Fig. 7. Influences of interface recombination velocity on QE of transmission-mode photocathode.

Figure 7 shows that when the interface recombination velocity is $S_v \leq 10^5$ cm/s, the cathode QE almost has no attenuation. When the interface recombination velocity is $S_v \geq 10^7$ cm/s, the cathode QE begins to decay significantly, especially the short wavelength efficiency, because short wavelength radiation is mainly absorbed near the interface and its photoemission is more easily influenced. The QE curve of our prepared GaN photocathode shown in Fig. 6 is flat and has uniform high emission efficiencies for both short and long wavelengths, which is consistent with the photoemission with a smaller interface recombination rate, as shown in Fig. 7. Using Eq. (1), the experimental curve shown in Fig. 6 was further fitted to assess the parameters of the cathode material and process. Curve fitting results show that the interface recombination velocity of our prepared cathode is 5×10^4 cm/s, achieving negligible magnitude, which proves that the design of the graded buffer layers is efficient in improving the interface quality between buffer and emission layers of the transmission-mode GaN photocathode. The improvement of the interface quality is also beneficial in obtaining high efficiency photoemission.

In conclusion, we have designed a transmission-mode GaN photocathode based on graded $Al_xGa_{1-x}N$ buffer layers, and successfully conducted photocathode preparation and photoemission characterization. Compared

with the transmission photocathode with an AlN buffer, this new type of transmission-mode UV photocathode has a higher QE and more flat responses of short and long wavelength UV. The graded buffer layer helps reduce the interface growth stress between buffer and emission materials, making these results beneficial to the improvement of optical emission performance. The graded buffer structured GaN photocathode will help promote the development of UV detection.

This work was supported by the National Natural Science Foundation of China under Grant No. 60701013.

References

1. Y. Zhang, K. Chu, X. Shao, Y. Yuan, D. Liu, X. Chen, and X. Li, Acta Opt. Sin. (in Chinese) **29,** 3515 (2009).
2. M. Zhao, J. Li, X. Wang, M. Zhou, J. Bao, and F. Gu, Acta Opt. Sin. (in Chinese) **29,** 3409 (2009).
3. J. Stock, G. Hilton, T. Norton, B. Woodgate, S. Aslam, and M. Ulmer, Proc. SPIE **5898,** 58980F (2005).
4. O. Siegmund, J. Vallerga, J. Mcphate, J. Malloya, A. Tremsin, A. Martin, M. Ulmer, and B. Wessels, Nuclear Instr. Methods in Phys. Res. A. **567,** 89 (2006).
5. J. Qiao, B. Chang, X. Du, J. Niu, and J. Zou, Acta Phys. Sin. (in Chinese) **59,** 2855 (2010).
6. A. M. Dabiran, A. M. Wowchak, and P. P. Chow, Proc. SPIE **7212,** 721213 (2009).
7. O. H. W. Siegmund, A. S. Tremsin, J. V. Vallerga, J. B. McPhate, J. S. Hull, J. Malloy, and A. M. Dabiran, Proc. SPIE **7021,** 70211B (2008).
8. X. Du, B. Chang, Y. Qian, R. Fu, P. Gao, and J. Qiao, Chinese J. Lasers (in Chinese) **37,** 385 (2010).
9. J. Qiao, B. Chang, S. Tian, X. Du, and P. Gao, Acta Phys. Sin. (in Chinese) **58,** 5847 (2009).
10. X. Du, B. Chang, Z. Zong, and Y. Qian, Opto-Electron. Eng. (in Chinese) **29,** (suppl.) 55 (2002).